

Simulating interactions of microrobots designed for pollutant removal in wastewater caused by the textile industry

D. Martinez¹, Asesores: C. Vélez Cuervo², J.F. Osma³

¹df.martinezv@uniandes.edu.co, ²cvelezcu@uci.edu, ³jf.osma43@uniandes.edu.co
Jun 2021

Resume – In this work we successfully made the design and magnetic simulations of forces of a microrobot with the structure of a gripper, done for the removal of contaminants from wastewaters generated by the textile industry. This microgripper works by closing itself and capturing contaminants. We made two types of studies, the first one is a Multiphysics simulation using COMSOL Multiphysics, on this software we analyzed the behavior of the magnetic field, the magnetic flux density and the magnetization. In addition, we developed an Analytical study using MATLAB. In this study we analyzed the magnetic forces that are present on the system such as repelling and attracting forces and the magnetic torque. With the results produced we analyzed the potential interactions of the microrobots and described the magnetic behavior. We successfully described by simulations and analytically the feasibility of the physical implementation.

Keywords –*microrobots, pollutant, magnetics, dyes, phenols, wastewater, magnetic force, torque, magnetic flux density.*

I. INTRODUCTION

The treatment of wastewater is essential because many of these are discharged directly into bodies of water such as rivers without any type of pretreatment, this causes great damage not only to the water source itself, but also affects different ecosystems present around it. From these sources altering the balance of both the biotic and abiotic environments [1]. These wastewaters present chemical, biological, organic pollutants, among others. Which generates great difficulty in its treatment and decontamination [2].

In industrial wastewater, there is contamination due to synthetic dyes or azo-type dyes, because these are produced in large quantities for use in different areas and their production can reach up to 75 tons per year [1] [3]. These azo-type dyes can affect the development of aquatic life once it enters different types of water, since they generate depletion of dissolved oxygen and interfere with photosynthetic processes [4]. Additionally, azo-type dyes cause damage to human health if there is a long exposure due to the different biotransformation that they can present, one of them is the release of aromatic amines which are absorbed by the skin causing mutations, and developing diseases such as cancer or neurological disorders [1] [5] [6].

In addition, one of the industries that most use this type of dye is the textile industry and because the fixation of the dye with the fibers is not complete, the use of these is very high, producing 200 billion liters per year of wastewater effluents. the

textile industry [7]. Currently, there are more than 9000 types of dyes of which the chemical structure of 896 azo dyes incorporated in the industry is known and only 426 have main compounds of 22 regulated amines, the rest present an exclusive metabolism with unregulated amines [5]. For this reason, different dye treatments have been developed in which physical and chemical methods have been applied, such as coagulation/flocculation, precipitation, ion-pair extraction, photocatalysis, ozonation, ultrasonic mineralization, among others [1]. The problem with these treatments is that they are expensive and given the wide range of dyes, they are not always effective. On the other hand, due to their low biodegradability, treatment of contaminated water with dyes different from conventional biological treatments such as membrane filtration or treatment with flocculants should be sought [1] [8].

Due to this, there is a need to propose a solution for the removal of azo dyes. Carrying out a dye removal approach in phenolic synthetic wastewater, this solution proposes the manufacture of microrobots. These micro robots are small machines that can reach places that are difficult to access and carry out different functions in different environments and areas of science [9] [10]. Additionally, these microrobots work with enzymatic components such as the laccase enzyme, which oxidizes phenolic compounds present in water [1]. These enzymes are part of the family of blue copper oxidoreductases found in fungi, which are capable of degrading aromatic amines [11] [12]. On the other hand, the microrobots will be composed of ferrous magnets and nickel. These magnets are floating on the sheet or surface of the phenolic water in direct contact with the laccases and thus carry out the process of oxidation of phenols and reduction of concentrations of azo-type dyes.

Finally, it is sought that, with the help of electromagnetism, once the laccases reach an inflection point and their oxidative efficiency is reduced, it is proposed to fold these microrobots with the help of an external magnetic field changes and in this way to be able to sediment them to subsequently remove them from the phenolic water.

II. MATERIALS AND METHODS

Before physical implementation of the microrobots. It is highly important to understand the behavior of the system and how it will act in uncontrolled scenarios and applications,

regardless of the situation the microrobots will be put on, they should work the way they need, this is because a little change in the mechanism and the response could end in an even worst case of contamination. Some simulations have to be done in order to have a clear response of how the mechanism will work. In addition to that, simulations can help with the exact measurements and geometries to have an optimal response in the real-world implementation.

The materials and methods are divided into several stages. First, there is a need to design a structure for the microrobots this general shape will give the initial taught of the model and it will open the path for future work.

A. General structure - description

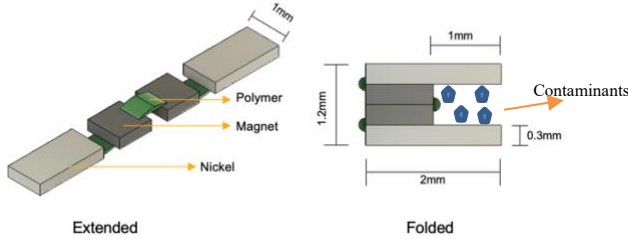


Figure 1. General structure microrobot. (Left) full structure open, where light gray rectangles correspond to the nickel pallets and darker gray squares represent the magnets. All structure is attached with polymeric strips. (Right) Folded microrobots.

Having a general structure, we can analyze some aspects and the right way to start with the simulation. First of all, here we have an array of ferromagnetic components. So, there is a need of using some key theories about magnetic interactions. Related with parallel magnetization. Also, a free body diagram is presented to analyze the forces that are implicated on this schema.

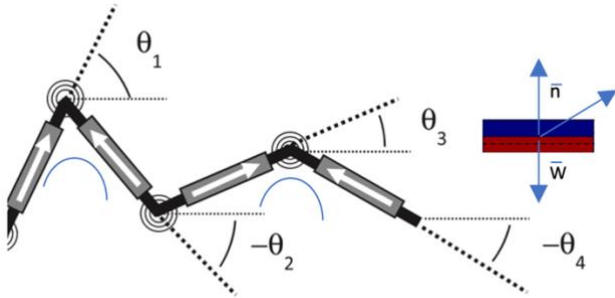


Figure 1b Intended flex of the microgripper. Image taken and adapted from [13]

The behavior of the microgripper is determined by its material properties (stiffness and magnetization), its structural geometry, and the applied magnetic field. Magnetic particles in the elastic composite experience forces F and torques t in the applied magnetic field B as.

$$F = (m \cdot \nabla)B \text{ and } \tau = m \times B$$

Where m and B are the magnetic moment and the magnetic flux density respectively [14]. More analytical process can be done but the mathematical model and equations are not in the

scope of this project. However, the references and additional info can be checked I

B. COMSOL Multiphysics simulations

Multiphysics simulations and analysis of this type of structure are highly important in a way that it can show the physical interactions of the objects. In this case we are using the AC/DC module from COMSOL Multiphysics with the study of current free magnetic interactions between two different ferromagnetic materials such as iron oxide and nickel. In this type of current free simulations, we know that.

$$\nabla \times H = 0$$

And it is possible to define the scalar magnetic potential, V_m , from the relation.

$$H = -\nabla V_m$$

This is analogous to the definition of the electric potential for static electric fields. Using the constitutive relation between the magnetic flux density and magnetic field.

$$B = \mu_0(H + M)$$

Together with the equation

$$\nabla \cdot B = 0$$

We can derive an equation for V_m

$$-\nabla \cdot (\mu_0 \nabla V_m - \mu_0 M_0) = 0$$

The model uses this equation by selecting the Magnetic Fields, No Currents interface from the AC/DC Module. And this will give us the interaction of the system by studying its scalar magnetic potential.

With the above theory it is possible to study the magnetic behavior of our system. Magnetic field studies, magnetic flux density and magnetization analysis can be achieved. The way we can do this is by. First, analyzing the BH curves of the magnets, in this way it is possible to set a schema for the base behavior of the system based on its natural magnetization response.

After the study of the BH curves is done, then the analysis is all done via COMSOL. First, we define the geometry of the system, using 3D modeling tools given by the software. Second, the definition of the materials must be done. With the BH curves we can define a magnetic behavior of the magnets. The nickel is defined using the integrated materials library included in the software. It is important to have in mind that the BH curves used in these simulations are taken from the K&J magnetics main page, due to the global situation, magnetic characterizations using VSM could not be done.

Having the definition of the materials, the next steps were related to the main simulation and graphic representation of the results. The Mesh definition, boundaries and general studies were done.

C. MATLAB Simulations

With studies developed a few years ago Janssen [15], Yonnet and Allag [16]. We know that it is possible to calculate the force between any two cuboid magnets with arbitrary magnetization directions. However, since the model produced by the research ended up having great results, it represents a huge amount of time to implement and analyze by hand. So, because if that, we used the public framework of verified and tested MATLAB code to calculate the forces between arbitrarily magnetized magnets. With a set of pre-defined functions that are provided to easily calculate the forces between arbitrary multipole arrays of magnets. The code is free access and can be used and modified for anyone.

This model is based on the theory for the study of an array of magnets interacting with each other that consist in a fixed ferromagnetic material and a floating one, just as can be seen on figure 2.

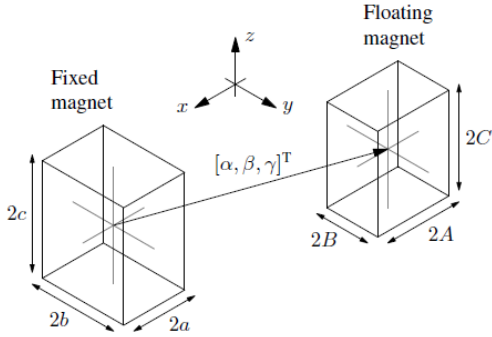


Figure 2. Depiction of the geometry for the two-magnet system taken from [15,16]

The geometry of the two-magnet system is shown in Figure 2, in which the magnets have side lengths $s = [2a, 2b, 2c]$ T and $S = [2A, 2B, 2C]$ T respectively and the distance between their centers is given by $d = [\alpha, \beta, \gamma]$ T.

The calculations always assume that the first magnet is fixed, and force is acting on the second magnet. The signs must be reversed to obtain the forces acting on the first magnet. Akoun and Yonnet provide the force expressions for magnets with vertical magnetization. This force is denoted herein as $F_{(z,z)} = (S, s, d, J_1, J_2)$ as a function of the magnet sizes, the distance between them, and their magnetization magnitudes J_1 and J_2 . Allag, Yonnet, and Latreche provide the force expressions for the first magnet with vertical magnetization and the second magnet with magnetization in the horizontal y direction. This force is denoted herein as $F_{(z,y)} = (S, s, d, J_1, J_2)$. The force between a vertically magnetized magnet and one with magnetization in the horizontal x -direction can be calculated by applying a rotational transformation to $F_{(z,y)}$ around the z -axis. That is

$$F_{(z,x)} = (S, s, d, J_1, J_2) \\ = R_z \left(-\frac{\pi}{2} \right) F_{(z,y)}(S_{(z,x)}, s_{(z,x)}, d_{(z,x)}, J_1, J_2)$$

Where $S_{(z,x)} = abs \left(R_z \left(\frac{\pi}{2} \right) S \right)$, $s_{(z,x)} = abs \left(R_z \left(\frac{\pi}{2} \right) s \right)$ and $d_{(z,x)} = R_z \left(\frac{\pi}{2} \right) d$. Using the force expressions $F_{(z,x)}$, $F_{(z,y)}$ and $F_{(z,z)}$ in superposition allows the force to be calculated between a vertically magnetized magnet and another magnet with arbitrary magnetization direction. By applying coordinate system transformations to these expressions, arbitrary magnetization directions can be achieved for the first magnet as well. Achieving that the force between two magnets of arbitrary magnetization can be written as follows

$$F = (S, s, d, J_1, J_2) = \sum_{(i,j) \in (x,y,z)^2} F_{(i,j)}(S, s, d, J_1, J_2)$$

Where:

$$J_1 = [J_{1x}, J_{1y}, J_{1z}]^T \text{ and } J_2 = [J_{2x}, J_{2y}, J_{2z}]^T$$

The theory presented in the equation above was implemented in the MATLAB code which perform the simulation of the magnetic force between the two magnets.

III. RESULTS

A. COMSOL Results

After the given theory of the simulations and having in mind the capability of COMSOL the simulations were done, and the results can be seen on figure 3. Here we have a couple of results of the simulations.

First, we have the main implementation of the microrobot. A general structure with four main parts. Two rectangles representing the nickel pallets and two square parts noted as iron pallets. We defined the materials in the COMSOL console and established all the studies needed. This general structure helped us to visualize the geometry of the micro robots easily. Figure 3a. Give this geometry we defined the mesh and the further analysis that could be done.

The first result is shown in figure 3B. Represents the interaction between the two magnets and the nickel pallets. Here we have three main results. On the top presented with the contour lines there is the magnetic flux density of the hole structure. It can be seen a clear interaction between the magnets and the nickel. The magnetic flux density gives us a general ideal of how the magnetic field in behaving on the micro robot.

On the other hand, represented by the straight lines if the magnetization, the nickel pallets are getting magnetized. It can be confirmed on the figure on the left, where the iso surface representing the magnetization and the magnetic flux density. In addition, on the figure of the bottom right there is a representation of the magnetic field on the hole structures as an iso surface. Here we can see the magnetic field lines also being present, this representation will help us to understand the further interaction of each of the micro robot parts.

On figure 3C. can be seen the study of the interaction between the two magnets and magnet with nickel. In this case, we wanted to study the response of the magnetic field and the

magnetic force between each of the parts. On the figure 3C the two lines represent the magnetic force exerted on the system. These results helped us to identify the peak forces of attraction and repulsion as a function of the separation of each of the parts. This analysis will help us to identify and choose the optimal separation between the magnets and the nickel to achieve a better result in terms of interaction and magnetic forces. Moreover, it will help with further torque analysis.

behavior of the magnetic circuit generated here. If we have a clear idea of the component of the magnetic field, we can develop a further study of the control of the microrobots based on magnetic theory and controlled external magnetic fields. These results returned a base of the behavior of the system without external magnetic interaction.

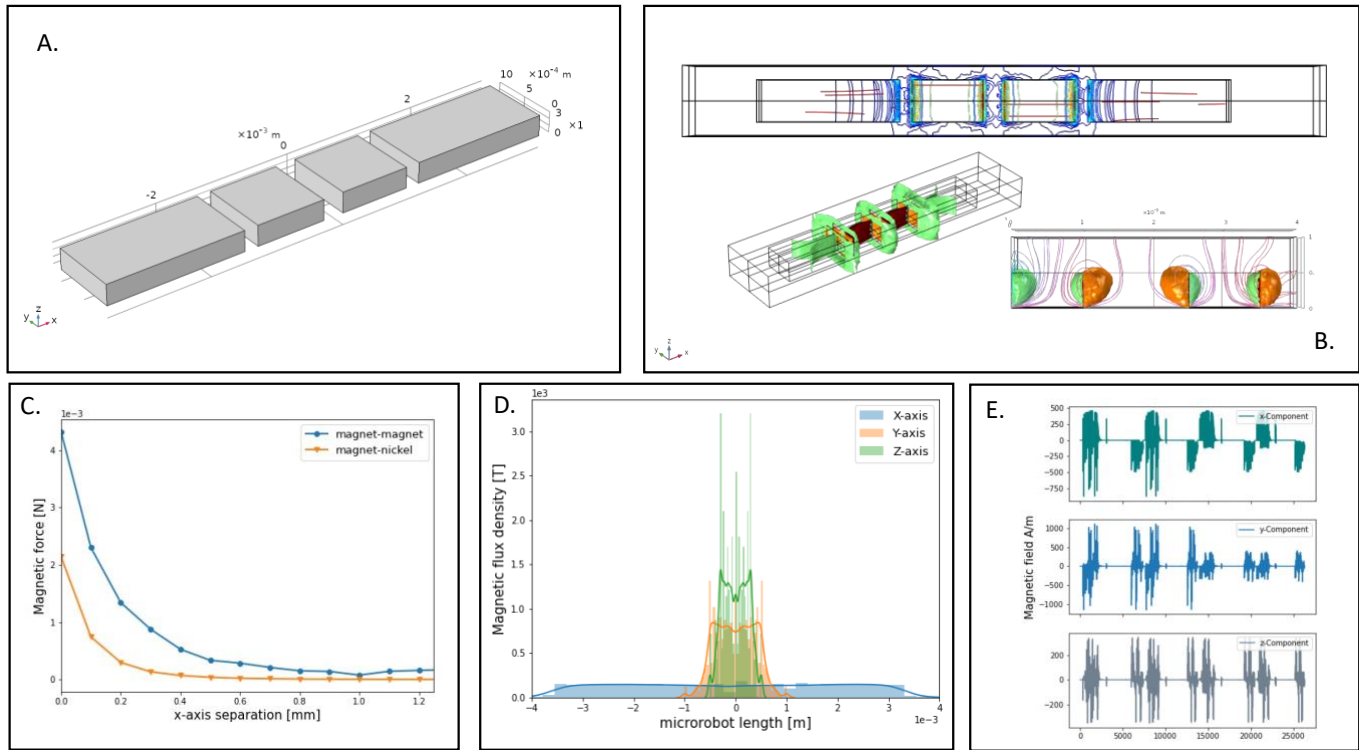


Figure 3. COMSOL results for a given structure on A. the general structure of two magnets (squares) and two nickel pallets (rectangles), the materials were defined using BH curves for the magnets and library included nickel material for the pallets. B. 3D results representing the magnetic flux density and magnetization (top) the magnetization and magnetic interaction (left) and the magnetic field (right). C. Analysis of the magnetic force between the two magnets and the magnetic force between a single magnet and a nickel pallet. D. Magnetic flux density of the whole structure of the micro robot divided by components. E. Magnetic field visualization on each geometric component along the structure of the micro robot.

B. MATLAB Results

In addition to the magnetic force, we also studied the magnetic flux density response of the system as can be seen of figure 3D. Here we analyze the components of the MF density (x, y and z components). The distribution of the density through the hole geometry of the micro robot is shown. From -4 mm to 4 mm, where 0 is the center of the system (between the two magnets). On the x component of the magnetic flux density, it can be seen a homogeneous distribution along the geometry, whereas on the y and z components the density is main located on the middle of the structure. Although the x axis is homogeneous, the density is lower than on other components. The z component of the magnetic flux density with the higher values but with a more centered distribution mainly focus on the part of the microrobots where the magnets are.

Finally, we made a study of the magnetic field components along the whole structure of the micro robot. Here we have three different figures showing each of the components of the magnetic field. These results will help us to understand the

Small and thin magnets can be difficult to obtain and hard to work with. While multiple smaller magnets can be stacked together to approximate a single large magnet, greater forces can be achieved by varying the magnetization pattern between adjacent magnets in the stack [15,16].

Having said that, we wanted to study the interactions between those smalls' parts in separate conditions. First, we started with the simulation of the repulsive force between the two magnets in the middle of the microrobots. And then se simulated the magnetic torque on the system. All the results can be seen on figure 4.

The first general geometry and structure was generated in order to see easily the geometry and the possible ways it can be modified. On figure 4 A there is a 3D generated structure on MATLAB. The green rectangles represent the nickel pallets which have a size of 2mm x 1mm and the blue/red squares represent the magnets with a magnetization directed on the z

axis. The separation between each one of the components is 0.5mm and will be filled on a further implementation with a flexible non-magnetic material.

In addition, on figure 4B, we have a profile of the hole structure, so the geometry, the dimensions and the separation can be seen easily. Here also we can see the height of the micro robots which is 0.3 mm.

analyze how the micro robot will perform when a flex is applied and if the main objective of this geometry is achieved.

Finally, having the COMSOL results in mind. We made a simulation of how the magnetic repulsion/attraction force will interact in the hole structure. As well as in the figure 4E. On figure 4 F. we have the graphs of the magnetic force exerted by each pair of components of the micro robot. With the analysis

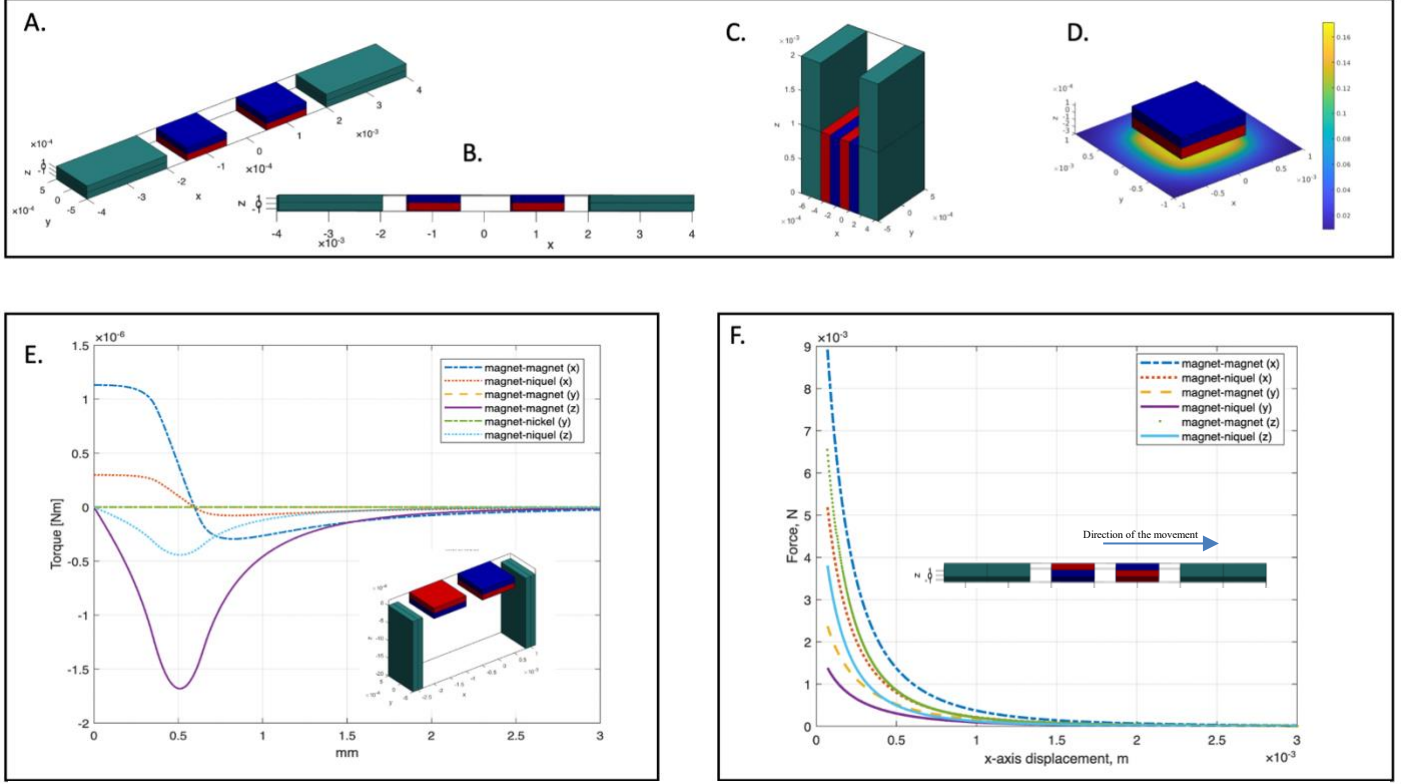


Figure 4 General figure for the MATLAB results obtained for the micro robot. Figures A,B and C represent the structure of the microrobot and how it will be folded form to capture contaminants. Where the green rectangles represent the nickel pallets and the blue/red squares the magnets. On figure E there is an analytical result of the magnetic torque of the structure, when it is folded at 90 degrees as shown on the figure and the force that is generating the torque in exerted on the direction of the movement. The figure F represents the magnetic force that is measured as a function of the separation between the following magnet-magnet and magnet-nickel. The separation occurs on the x-axis.

We also wanted to study the behavior of the folded form of the micro robot. This forms the gripping that will be performed when a change of the external magnetic field interacts with the micro robot. However, this topic will be studied later. This can be seen of figure 4 C.

Having the 3D structures generated with the correct properties we proceed to analyze the magnetic field of a single magnet. On figure 4 D. there is a representation of how the magnetic field of a single magnet can be represented. This helped us seeing that the properties were applied, and the magnetic interaction can be achieved.

With the structured and the equations on MATLAB to do the simulations we started to develop two main results. The first one, on figure 4 E we have the results of the magnetic torque exerted by the structure when it is at 90 degrees as can be seen on the 3d graph inside the graph. We plotted the magnetic torque of each of the pair of pallets. Magnet and nickel on all the axis the force can be analyzed. This result will help us to

of all the axis present. The Ideal for this graph is so match the results. We had on the COMSOL simulation, and this will help us to analyze the behaviors of our system in terms of the force that can be achieved.

This results on MATLAB will help the analysis and the development of how to control this microrobots. And to see and understand the geometry and if it achieves what the need are.

IV. ANALYSIS

Having the results from the section above, it is possible to generate a series analysis in order to understand the behavior of our system and what could be the expected results when a physical implementation could be done. With the two main results we achieved, using COMSOL and MATLAB, it is possible to complement the idea of the description of the magnetic behavior. However, it is important to say that the two results, simulation and analytical analysis were intended to

achieve different goals, the information we got can be used to generate a well-structured analysis.

When it comes to the COMSOL results, we have a couple of point to talk about. First, in figure 3B it is possible to see 3 different results regarding of magnetic behavior of the microgripper. The top figure represents the combined results of the magnetic flux density (blue lines) and the magnetization (red lines). On this figure the magnetic flux density is focused on the joints between each of the component of the microgripper. We can see how, between the two magnets, on the middle of the structure, we have a greater amount of magnetic flux density lines. As it is known, the magnetic flux density represents the strength and the direction of the magnetic field around a magnet of a ferromagnetic element. It can be seen also, the presence of the magnetic flux density lines where the nickel pallets are located. This goes by the hand with the magnetization lines located inside the nickel pallets.

The magnetization lines observed on the figure represent how the magnets generate a magnetic flux with the nickel pallets. It can be seen also on the two representations bellow. Where the magnetic flux density and the magnetic field are shown as 3D surfaces. There is a magnetic field measured at each of the rectangles of the structure. Having the higher values of the magnetic field on the magnets and the smaller ones with the nickel pallets.

Apart from the magnetic flux density and the magnetic field, the results of the magnetic force between each part of the microgripper is shown on figure 2c. The forces were analyzed, first with two magnets and then a magnet and a nickel pallet. The idea was to understand the behavior of the forces and magnetic field when then pieces were separated on the x-axis. The measurements were taken by leaving a component still and moving the other one on the opposite direction. From the results on figure 3c. The force between the two magnets was clearly greater than the forces between the magnet and the nickel pallet. This result showed us that on the middle of the microrobot, there is a force that is stronger than the other from the rest of the micro robots. In addition to that, we found that when the separation on the x-axis is greater than 0.6mm, in the case of the magnet-nickel setup, the magnetic force approaches to zero, which means that the interaction between those elements is lost and they are not working together as a single device. However, when it comes to the interaction between the two magnets, the point where the force decreases are greater than 1.2mm. This is important because when the final implementation would be done, we must choose a distance between each part of the microrobot that helps achieving better results. This distance will be chosen when the MATLAB results are analyzed in order to have a complete analysis.

On the other hand, figures 3D and 3E, are results related with the magnetic flux density and the magnetic field of the structure. These results helped us to determine how the distribution of the field is on the structure and where to focus when studying the torque analysis. First, figure 3D is a representation of the magnetic flux density along the structure

of the micro robots. Being 0 the center of the structure, between the two magnets and -4 and 4 the two boundaries.

When analyzing the distribution of the magnetic flux density on the 3 axes when we talk about the x-axis, the distribution is homogeneous along the whole structure, having a constant 0.2T. This represents that, in fact, the magnetic field on the x-component is homogeneous. As can be seen on figure 2 E. Where the graphs showing the magnetic field stays the same during the measurement, we have spikes between -500 and 500 A/m repeating. This result gives us the information that, in fact the microrobot can be stay expanded without any external force actuating on the x-axis.

However, when we see on figure 3D, the distribution of the magnetic flux density corresponding to the z-axis. Here we have a focused distribution of the magnetic flux density on the middle of the structure, as well as on the y-axis. This kind of distribution represents the magnets on the middle, and the magnetic field they are producing. We can study with this that the magnetization we are producing over the nickel pallets is not generated on all axes. So, the magnetic field of the magnets overlaps and the presence of other magnetic fields on the structure are lower on these axes. This can be analyzed also seen the results on figure 3E. when then magnetic field is not homogeneous, and the distribution of the spikes is non-homogeneous either.

The COMSOL analysis helped us to identify the general magnetic behavior of the microgripper. However, the description we need to do, in order to understand the real functionality of the design, must be complemented with some analytical results for the magnetic forces presents in the system.

Having said that, the results from MATLAB analysis were resumed on figure 4. These results are focuses on the magnetic torque and the magnetic forces of the system based on the analytical model by Janssen, Yonnet and Allag in 2009. However, before to the analysis, on figures 4A,B and C there is a 3D representation of the structure and the folding final form of the microrobot as discussed on the beginning of this document. The representation expresses how the contaminants will be gripped and removed away from the water. On the other hand, figure 4D represents a model generated with the code to show the magnetic field of a single magnet with magnetization on the z axis. So, we are sure the generation of the structure is correct.

In addition to that, on figure 4E, there is a result of the magnetic torque of the system. This torque was analyzed by generating a fold on the structure such as how it will be when is 90 degrees tilted. On this analysis, we studied the relation between 2 systems. Magnet-magnet and , magnet-nickel. With one of the two tilted 90 degrees. And moved on the x axis. The force exerted in order to generate the torque going on the direction of the folding. At this point we wanted to analyze the relation between the separation of the parts and how the magnetic torque would be behaving. Based on figure 4E, we discovered that. The magnetic torque on the z-axis between the two magnets is 3 times higher than the torque on the z-axis between the magnet-nickel system. This goes with the theory, since the soft

magnetic material does not interact as the magnet and hence, the magnetic torque measured is lower. The key point to see here is that when the separation between the pallets is 0.5 mm we see a maximum absolute value of the torque, which means that at that distance we have the higher integration related to the torque. With $1.7\text{e-}6$ Nm for magnet-magnet and $0.5\text{e-}6$ Nm for magnet-nickel.

It is important to clarify that magnetic torque on the x-axis and this kind of interactions are the ones that give us the path to follow in order to understand the processing of folding the microrobot and how it would be controlled afterwards. This x-axis forces are lower in magnitude than the ones from the z-axis because of the direction of the force applied and the movement. Meanwhile the forces on the y-axis remain on zero. This makes sense with the theory since there is not movement on the y-axis during this simulation.

Complementing the results of the magnetic torque, we have the simulations of the magnetic force between the two same systems. Magnet-magnet and magnet-nickel. The objective here was to complement the results of the torque and the forces analysis made on the COMSOL results. As seen on past results, the focus here is on the x-axis force, having a peak value of $10\text{e-}3$ N for the magnet-magnet system and $5.3\text{e-}3$ N for the magnet-nickel. This results while is lower than the results from COMSOL, the magnitude stays the same and the scale also remains. These changes of the actual value have several causes, such as the size of the mesh from the COMSOL simulation, the material definition, the number of points taken among others. On these results, the point where the force starts to decrease to the point it is not relevant to the system, interaction below $0.5\text{e-}3$ N is located on 0.5mm of separation. After that point all the forces go to zero and the interaction is not relevant to the main propose of the microgripper. On this figure we also have the representation of the other axis, we can clearly see that no matter what is the axis we are studying, the results are continuous. When there is a magnet-magnet interaction, the force is increased than when there is a magnet-nickel analysis. It is possible to see too that the forces on the y-axis are lower, since there is not movement on this direction.

The advantage of having both, MATLAB and COMSOL helped us to identify the key point of the system and the geometry and helped understand how the magnetic behaviors of the microgripper are. The analytical results and the simulations were complementary to understand how the microrobot will perform under controlled external magnetic field, as well as helped us to improve the design and the geometry in order to take advantage of the points where the forces are stronger to improve the folding and capturing of the contaminants.

V. CONCLUSIONS

This project presents a new contribution for magnetic microrobots and its applications. These investigations and results allow the direct calculation of many systems working by the forces or the torques between magnetized elements.

These results can also be used for many other geometries, like complex shapes of magnets which can be replaced by a

combination of several soft ferromagnetic ones like nickel. These results can be applied to many magneto-mechanical applications, these analytical results also allow a simple optimization model of a specific new geometry.

In addition, the interaction forces exerted between a soft ferromagnetic and a strong ferro magnetic material have been calculated, by analytical and simulation means only. In order to have a better set of results and a generalized model, some physical implementation needs to be driven. Moreover, during this project we adapted some older code for the analytical results and developed, the code is stored and documented on a GitHub repository for public access.

We Successfully studied the behavior of the magnetic microrobots and analyzed the points where the geometry works on a physical and magnetic way. The interactions between each of the parts of the microrobots showed us that, in fact, it is viable to implement a prototype. Not only we analyzed the forces and the magnetic field on the structure, but we also studied the cause of those interactions and results, and that brings to the plan options, for example the usage of external magnetic field to control the actuation of the micro robots. With the analysis of the forces we made, we can understand how the external magnetic field need to be in order to generate a control over the actuation of the robots.

Finally, with the studies generated on this work, we opened the options of new projects to come, the studies of the magnetic microstructures on the region are just starting to rise. With this base of work and the compiled information with simulations some other projects can be started and develop a new field of study.

VI. FUTURE WORK

With the results from this job, it is possible to develop a publication that can be impactful on the scientific community. With a physical implementation, characterization of the components by VSM, and actual test of the removal efficiency, it is possible to create a referenceable paper and achieve an impact on the field of micro robotics.

When it comes to further projects, this work gives the base and the 'know how' to other students and researchers. There are several projects that can come after this. And that are currently on progress, like the analysis of the interaction of the microrobots with others, the control of the path and the actuation of it, the functionalization of the surface in order to achieve a better removal process. It also could be implemented a machine learning model to predict the path of the microrobots on a certain type of environment such as riven waters, sea, lakes among others.

The magnetic description is just the start of a series of project that could lead into a new field on innovation on the university of Los Andes.

VII. REFERENCES

- [1] S. Lee *et al.*, “~~濟無~~No Title No Title,” *J. Chem. Inf. Model.*, vol. 53, no. 9, pp. 1689–1699, 2012, doi: 10.1017/CBO9781107415324.004.
- [2] H. Abu Hasan, M. H. Muhammad, and N. I. Ismail, “A review of biological drinking water treatment technologies for contaminants removal from polluted water resources,” *J. Water Process Eng.*, vol. 33, no. May 2019, p. 101035, 2020, doi: 10.1016/j.jwpe.2019.101035.
- [3] A. Tkaczyk, K. Mitrowska, and A. Posyniak, “Synthetic organic dyes as contaminants of the aquatic environment and their implications for ecosystems: A review,” *Sci. Total Environ.*, vol. 717, p. 137222, 2020, doi: 10.1016/j.scitotenv.2020.137222.
- [4] R. D. G. Franca *et al.*, “*Oerskovia paurometabola* can efficiently decolorize azo dye Acid Red 14 and remove its recalcitrant metabolite,” *Ecotoxicol. Environ. Saf.*, vol. 191, no. August 2019, p. 110007, 2020, doi: 10.1016/j.ecoenv.2019.110007.
- [5] B. J. Brüscheiler and C. Merlot, “Azo dyes in clothing textiles can be cleaved into a series of mutagenic aromatic amines which are not regulated yet,” *Regul. Toxicol. Pharmacol.*, vol. 88, pp. 214–226, 2017, doi: 10.1016/j.yrtph.2017.06.012.
- [6] A. Das and A. Dey, “P-Nitrophenol -Bioremediation using potent *Pseudomonas* strain from the textile dye industry effluent,” *J. Environ. Chem. Eng.*, vol. 8, no. 4, p. 103830, 2020, doi: 10.1016/j.jece.2020.103830.
- [7] V. S. G. Garcia, J. M. Rosa, and S. I. Borrelly, “Toxicity and color reduction of a textile effluent containing reactive red 239 dye by electron beam irradiation,” *Radiat. Phys. Chem.*, vol. 172, no. February, p. 108765, 2020, doi: 10.1016/j.radphyschem.2020.108765.
- [8] N. Saravanan and K. S. K. Sasikumar, “Wastewater treatment process using Nano TiO₂,” *Mater. Today Proc.*, no. xxxx, pp. 10–12, 2020, doi: 10.1016/j.matpr.2019.12.143.
- [9] A. Halder and Y. Sun, “Biocompatible propulsion for biomedical micro/nano robotics,” *Biosens. Bioelectron.*, vol. 139, no. February, p. 111334, 2019, doi: 10.1016/j.bios.2019.111334.
- [10] Y. Wang, Y. Jiang, H. Wu, and Y. Yang, “Floating robotic insects to obtain electric energy from water surface for realizing some self-powered functions,” *Nano Energy*, vol. 63, no. April, p. 103810, 2019, doi: 10.1016/j.nanoen.2019.06.006.
- [11] X. Qiu, Y. Wang, Y. Xue, W. Li, and Y. Hu, “Laccase immobilized on magnetic nanoparticles modified by amino-functionalized ionic liquid via dialdehyde starch for phenolic compounds biodegradation,” *Chem. Eng. J.*, no. September 2019, doi: 10.1016/j.cej.2019.123564.
- [12] V. M. de Aguiar, R. Esquinelato Silva, R. A. C. Leão, R. O. M. A. de Souza, R. S. B. Gonçalves, and L. S. de Mariz e Miranda, “Studies on the laccases catalyzed oxidation of norbelladine like acetamides,” *Mol. Catal.*, vol. 485, no. February, p. 110788, 2020, doi: 10.1016/j.mcat.2020.110788.
- [13] Sheridan, R., Roche, J., & Lofland, S. E. (2014). Numerical simulation and experimental validation of the large deformation bending and folding behavior of magneto-active elastomer composites. *Smart materials and structures*, 23(9), 094004.
- [14] Zhang, J., & Diller, E. (2016). Tetherless mobile micrograsping using a magnetic elastic composite material. *Smart Materials and Structures*, 25(11), 11LT03.
- [15] H. Allag and J.-P. Yonnet, “3-D analytical calculation of the torque and force exerted between two cuboidal magnets,” *IEEE Trans. Magn.*, vol. 45, no. 10, pp. 3969-3972, Oct. 2009.
- [16] J. L. G. Janssen, J. J. H. Paulides, J. C. Compter, and E. A. Lomonova, “Three- dimensional analytical calculation of the torque between permanent magnets in magnetic bearings,” *IEEE Trans. Magn.*, 46, 1748 (2010).
- [17] E. P. Furlani, “Formulas for the force and torque of axial couplings,” *IEEE Trans. Magnetism*, vol. 29, no. 5, pp. 2295-2301, Sept. 1993.